

Forced Dynamics Control of the Elastic Joint Drive with Single Rotor Position Sensor

DOI 10.7305/automatika.54-3.160
UDK 621.532.8.03.015.4:621.313.13(621.828)
IFAC 2.1.4; 5.5.4

Original scientific paper

Position control system of moderate precision based on ‘forced dynamics control’ for the drive with significant vibration modes is described. To exploit the only position sensor on the motor side, all necessary control variables are estimated in observers based on motor position and stator current measurements. The designed controller is of a cascade structure, comprising an inner speed control loop, which respects vector control principles and an outer position control loop, which is designed to control load angle with prescribed dynamics in the presence of flexible modes. Simulations of the overall control system indicate that the proposed control system exhibits the desired robustness and therefore warrants further development and experimental investigation.

Key words: Forced Dynamics Control, Observers, Position Control, Sensorless Control

Prisilno upravljanje dinamikom pogona elastičnog zgloba s jednim senzorom pozicije rotora. U radu je opisano upravljanje sustavom pozicioniranja srednje preciznosti s izraženim vibracijskim modovima korištenjem metodologije prisilnog upravljanja dinamikom. Kako bi se iskoristio senzor pozicije na strani motora, sve potrebne varijable stanja estimiraju se na temelju mjerenja pozicije motora i statorskih struja. Projektirani regulator je kaskadne strukture, s unutarnjom petljom po brzini vrtnje koja se temelji na principima vektorskog upravljanja, i vanjskom petljom po poziciji za upravljanje kutom tereta s definiranom dinamikom u prisustvu slabo prigušenih modova. Simulacijski rezultati cjelokupnog sustava upravljanja potvrđuju da predloženi sustav upravljanja posjeduje željenu robusnost i time opravdava budući razvoj i eksperimentalna istraživanja.

Ključne riječi: prisilno upravljanje dinamikom, obzerveri, upravljanje pozicijom, bezsenzorsko upravljanje

1 INTRODUCTION

To reduce the number of sensors for position control of the drive with flexible coupling, a control system based on ‘Forced Dynamics Control’ (FDC) with measurement of rotor position and stator current torque component is developed. An overall control system is therefore completed with observation of all necessary control variables. Position control algorithm of the drive with torsion vibrations is developed in two steps.

Firstly, an inner speed control loop is formed for the PMSM rotor using feedback linearisation principles, [1]. This control algorithm is formulated in the rotor fixed d_q frame, respecting mutual orthogonality of the stator current vector and rotor magnetic flux vector, to achieve maximum torque under vector control [2-3]. Assuming a known load torque, FDC forces the speed control system to respond with a prescribed linear first order dynamic, which has a specified time constant, T_ω . This prescribed behavior of the speed control loop then enables to replace it with a first

order delay which substantially simplifies the design of the outer position control loop. Presence of the load torque estimate in the speed control algorithm automatically counteracts the load torque on the motor shaft by producing a nearly equal and opposite control torque component. Its estimate is provided by the motor torque observer. This gives FDC a certain degree of robustness not only with respect to external disturbances, but also with respect to plant parameter variations, since such variations are equivalent to load torques applied to the unperturbed plant model.

The second step is the design of the position control loop, which is also based on FDC and therefore complies with the prescribed closed-loop dynamics for load angle control, in spite of the presence of vibration modes and external load torque [4-5]. This approach achieves non-oscillatory position control with a settling time, T_{ss} , which can be described as a function of the natural frequency of two mass system.

Linearisation of the speed control algorithm and the design of the FDC based position control algorithm, operat-

ing with the motor position sensor only, require estimation of state variables including load torques. To achieve these tasks three observers complete the overall control system. State dependence of the flexible load variables is exploited to design their observer as a state observer. The second observer, which produces the first and second derivatives of the load torque is Luenberger's type and the reason for its separation from the state observer is to decrease order of the first one. The third observer is based on similar principles for estimation of load torque acting on the motor shaft for correct operation of FDC speed control loop.

Systematic analysis of speed control of the drive with flexible coupling with PI and PID regulators designed by pole-placement method is described in [6-7]. Analysis results in an important observation that the different pole-assignment patterns are necessary for the different inertia ratios between load and motor. If for an over damped system with a higher moment of load inertia PI regulator with specified damping coefficients satisfies non-oscillatory operation, then for highly under damped systems with load inertia lower than inertia of motor PID regulator is required to improve the control system performance.

An optimal speed controller design for a two inertia system stabilization based on 'The Integral of Time multiply by Absolute Error' criterion described in [8] results in analysis of four different controllers. Improvement of controller tracking performance was achieved with pseudo-derivative feedback and for better disturbance rejection a feed-forward controller is proposed.

A servo-system, which exploits the model of two-inertia system and Kalman filter based observer to predict one step ahead all state variables as well as disturbances, is described in [9]. Capability of the proposed algorithm to estimate and control the speed and position of the drive is verified by simulation with good results.

Possibility to exploit FDC for control of the drive with flexible coupling was already verified in [10-11]. Simulation results including preliminary experimental verification, confirm the effectiveness of the proposed control method. These works have also confirmed that FDC is capable to control vibration modes while offering precisely defined dynamic response to the reference position.

FDC based control system designed in [12] requires two position sensors for rotor and load position measurements as the inputs of FDC position control law. Preliminary experiments confirmed the possibility to control rotor and load angle with prescribed dynamics.

Further study based on simulations, verifies the ability to control the drive with flexible coupling with rotor position and current torque component measurements only. The control algorithm fed by observed state variables including torque on the motor shaft and load torque oper-

ates in agreement with theoretical assumptions made during its development. Results of simulations confirmed that the designed control system is capable to eliminate the influence of flexible coupling while controlling the load position with moderate precision.

2 CONTROL LAW DEVELOPMENT

Development of the position control system is made in two steps. At first the speed control system is linearised to achieve the first order response to the step angular speed demand [13]. Secondly, FDC position control system with prescribed closed-loop dynamics is designed. If compared with previous works the designed observers require measurements of rotor position and torque component of stator current. This way elimination of position sensor on the side of load was achieved.

2.1 Description of PMSM and Flexible Load

As a driving motor PMSM is supposed and its description in the synchronously rotating d_q co-ordinate system fixed to the rotor is as follows:

$$\frac{d\theta_R}{dt} = \omega_R, \tag{1}$$

$$\frac{d\omega_R}{dt} = \frac{1}{J_R} [c(\Psi_d i_q + \Psi_q i_d) - \Gamma_{Ls}], \tag{2}$$

$$\frac{di_d}{dt} = \frac{-R_s}{L_d} i_d + p\omega_R \frac{L_q}{L_d} i_q + \frac{1}{L_d} u_d, \tag{3}$$

$$\frac{di_q}{dt} = \frac{-R_s}{L_q} i_q - p\omega_R \frac{L_d}{L_q} i_d - \frac{p\omega_R}{L_q} \Psi_{PM} + \frac{1}{L_q} u_q, \tag{4}$$

where i_d, i_q and u_d, u_q are, respectively, the stator current and voltage components, L_d, L_q are, respectively, the inductances in direct and quadrature axis R_s is resistance of stator phase, θ_R and ω_R are the rotor position and angular velocity respectively and Γ_{Ls} is the external motor torque, p is the number of pole pairs and $c = 3p/2$ and J_R is the rotor moment of inertia.

Flexible coupling between motor and load for its description is shown in Figure 1.

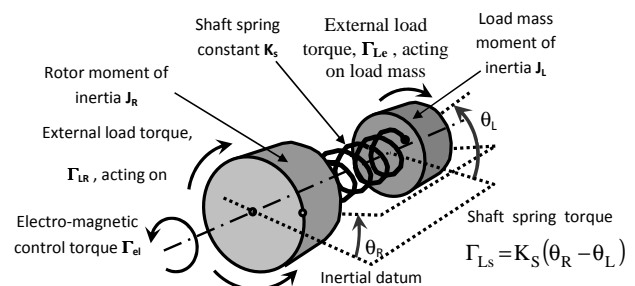


Fig. 1. Flexible coupling between motor and load

The driven mechanism is a balanced mass with moment of inertia J_L , coupled to the motor shaft via a torsion spring representing the flexible coupling with spring constant, K_S . The electrical torque developed by the motor is Γ_{el} . Γ_{Le} and Γ_{Ls} are load torques externally applied, respectively, to the load mass and the rotor. The torque, Γ_{Ls} is direct proportional to the position displacement. Block diagram for flexible coupling representation is shown in Figure 2.

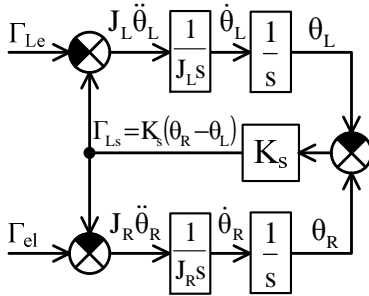


Fig. 2. Block diagram of flexible coupling

Mathematical description of flexible coupling between rotor and load is as follows:

$$\dot{\theta}_R = \omega_R, \quad (5)$$

$$\ddot{\theta}_R = \frac{1}{J_R} [\Gamma_{el} - \Gamma_{Ls}], \text{ where } \Gamma_{Ls} = K_s (\theta_R - \theta_L) \quad (6)$$

$$\dot{\theta}_L = \omega_L, \quad (7)$$

$$\ddot{\theta}_L = \frac{1}{J_L} [\Gamma_{Ls} - \Gamma_{Le}]. \quad (8)$$

Using Mason's formula the transfer function between the electrical torque and the rotor angle can be derived directly from Figure 2 as:

$$\begin{aligned} F(s) &= \frac{\theta_R(s)}{\Gamma_{el}(s)} = \frac{s^2 + \frac{K_s}{J_L}}{s^2 J_R \left(s^2 + \frac{K_s}{J_R} + \frac{K_s}{J_L} \right)} \\ &= \frac{1}{s^2 J_R} \frac{s^2 + v_n^2}{s^2 + \omega_n^2} \end{aligned} \quad (9)$$

where:

$$v_n = \sqrt{\frac{K_s}{J_L}} \text{ and } \omega_n = \sqrt{\frac{K_s}{J_R} + \frac{K_s}{J_L}} = v_n \sqrt{1 + \frac{J_L}{J_R}} \quad (10)$$

Here, the 'encastre natural frequency', v_n , is the frequency of the oscillations of the spring and load with the rotor held inertially fixed and with $\Gamma_{Le} = 0$. The 'free natural frequency', ω_n , is the frequency of the oscillations of the combined rotor, spring and load with $\Gamma_{Le} = 0$ and $\Gamma_{el} = 0$.

2.2 FDC of Motor Speed

FDC law for rotor speed is based on the feedback linearisation that yields the first order linear dynamics, where T_w is the prescribed time constant and $\dot{\theta}_{Rdem}$ is the demanded rotor speed

$$\ddot{\theta}_R = \frac{1}{T_w} (\dot{\theta}_{Rdem} - \dot{\theta}_R). \quad (11)$$

Linearisation is achieved through comparison of equation for prescribed dynamics, (11) with equation for rotor speed, (2). Setting $i_d = 0$ up to nominal speed for vector control of the PMSM, [2] and equating the RHS of (2) and (11) yields the following FDC law for speed control loop:

$$\begin{aligned} i_{d dem} &= 0, \\ i_{q dem} &= \frac{1}{c\Psi_{PM}} \left[\frac{J_r}{T_w} (\dot{\theta}_{Rdem} - \dot{\theta}_R) + \Gamma_{Ls} \right] \end{aligned} \quad (12)$$

hence $i_d = i_{d dem}$ and $i_q = i_{q dem}$ are regarded as the control variables. A current controlled inverter is used to vary the stator voltage components, u_d and u_q , in such a way that stator current components i_d and i_q follow their respective demands, $i_{d dem}$ and $i_{q dem}$, with nearly zero dynamic lag.

Since the motor load torque, Γ_{Ls} appears on the right hand side of the demanded current, $i_{q dem}$, (12) it is necessary to design an observer for estimation of the net load torque on the shaft of the motor (see section 3.3). Derived stator current demands (12) are used for FDC of PMSM rotor speed with the first order dynamics and prescribed settling time, T_w as it requires prescribed linearising function (11).

2.3 Design of Load Position FDC

To design the prescribed response for a control system with n closed loop poles having equal real parts, $-1/T_c = \omega_0$, and with a specified settling time, T_s , then the Dodds settling time formula, [14] applies. If zero overshoot of the step response is required, then:

$$\frac{y(s)}{y_{dem}(s)} = \left[\frac{1}{1 + sT_s/1.5(1+n)} \right]^n \quad (13)$$

where $y(s)$ is the controlled output and $y_{dem}(s)$ is the reference input. This formula is valid for the design of FDC speed control algorithms as well as for the design of load angle control algorithm of the drive with flexible coupling.

Plant for load position control is formed by the first order transfer function block representing FDC of rotor speed completed with kinematics integrator and integrating these blocks with the model of load. The resulting plant is shown in Figure 3. Load torque acting on the rotor shaft

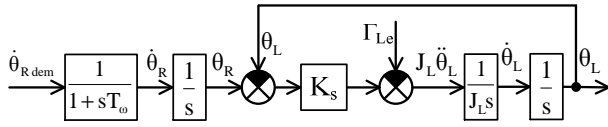


Fig. 3. Block diagram for load angle control

does not appear because it has been cancelled in the speed FDC loop.

Successive differentiation of (8) combined with (6) gives:

$$\ddot{\theta}_L = \frac{1}{J_L} [K_s (\dot{\theta}_R - \dot{\theta}_L) - \dot{\Gamma}_{Le}], \quad (14)$$

$$\theta_L^{IV} = \frac{1}{J_L} [K_s (\ddot{\theta}_R - \ddot{\theta}_L) - \ddot{\Gamma}_{Le}]. \quad (15)$$

Substituting in (14) for $\ddot{\theta}_R$ from (11) and for $\ddot{\theta}_L$ from (8) yields for load angle control following 4th order equation:

$$\theta_L^{IV} = \frac{K_s}{J_L T_\omega} (\dot{\theta}_{R dem} - \dot{\theta}_R) - \frac{K_s^2}{J_L^2} (\theta_R - \theta_L) + \frac{K_s}{J_L^2} \Gamma_{Le} - \frac{1}{J_L} \ddot{\Gamma}_{Le}. \quad (16)$$

Using (13) for $n = 4$, the following 4th order system will yield a specified settling time, $T_{s\theta}$:

$$\frac{\theta_L(s)}{\theta_{L dem}(s)} = \frac{\left(\frac{15}{2T_{s\theta}}\right)^4}{A(s)}, \quad (17)$$

$$A(s) = s^4 + 4\left(\frac{15}{2T_{s\theta}}\right)s^3 + 6\left(\frac{15}{2T_{s\theta}}\right)^2 s^2 + 4\left(\frac{15}{2T_{s\theta}}\right)^3 s + \left(\frac{15}{2T_{s\theta}}\right)^4.$$

The comparison of the 4th derivative (16) of load position, θ_L , with prescribed position (17) results in:

$$\frac{K_s}{J_L T_\omega} (\dot{\theta}_{R dem} - \dot{\theta}_R) - \frac{K_s^2}{J_L^2} (\theta_R - \theta_L) + \frac{K_s}{J_L^2} \Gamma_{Le} - \frac{1}{J_L} \ddot{\Gamma}_{Le} + \frac{4}{b} \ddot{\theta}_L + \frac{6}{b^2} \ddot{\theta}_L + \frac{4}{b^3} \dot{\theta}_L = \frac{1}{b^4} (\theta_{L dem} - \theta_L), \quad (18)$$

where $\dot{\theta}_{R dem}$ is treated as the control variable and $b = 2T_{s\theta}/15$. By manipulation of (18) the following FDC

control law for load angle control is derived:

$$\dot{\theta}_{R dem} = T_\omega \left\{ \frac{J_L}{b^4 K_s} (\theta_{L dem} - \theta_L) + \frac{1}{T_\omega} \dot{\theta}_R - \frac{4}{b} (\dot{\theta}_R - \dot{\theta}_L) - \left[\frac{6}{b^2} - \frac{K_s}{J_L} \right] (\theta_R - \theta_L) - \frac{4J_L}{b^3 K_s} \dot{\theta}_L - \left[\frac{1}{J_L} - \frac{6}{b^2 K_s} \right] \Gamma_{Le} + \frac{4}{b K_s} \dot{\Gamma}_{Le} + \frac{1}{K_s} \ddot{\Gamma}_{Le} \right\}. \quad (19)$$

This control law also satisfies ideal transfer function:

$$F(s) = \frac{\theta_{L id}(s)}{\theta_{L dem}(s)} = \frac{1}{b^4 s^4 + 4b^3 s^3 + 6b^2 s^2 + 4bs + 1}. \quad (20)$$

The derived position control algorithm, (19) is in the form of a state feedback control law with the gains already determined as functions of the plant parameters and the desired closed loop system parameters (17). But in this case, the first and second derivatives of the external load torque also appear on the right hand side. This is a general feature of FDC when external disturbances are included into the plant model used for the control system synthesis. The designed overall control system is shown in Figure 4.

3 OBSERVATION OF CONTROL VARIABLES

All the state variables for the designed control law are generated by a state observer, which needs rotor position and stator current torque component as the inputs. For the estimation of external load torque derivatives an observer with filtering effect is designed. Load torque acting on the shaft of the motor is estimated in the motor torque observer.

3.1 Observer of State Variables

Due to state dependence of the deflection torque, Γ_{Ls} the ‘state variables observer’ is based on a real time model of the two-mass system, where Γ_{Le} is an external load torque. In this case the external torque is treated as if it is constant provided that its change over a period equal to the observer correction loop settling time T_{sO} is negligible. System state equations are:

$$s\theta_L = \omega_L, \quad (21)$$

$$s\theta_R = \omega_R, \quad (22)$$

$$s\omega_L = -\frac{K_s}{J_L} \theta_L + \frac{K_s}{J_L} \theta_R - \frac{1}{J_L} \Gamma_{Le}, \quad (23)$$

$$s\omega_R = \frac{K_s}{J_R} \theta_L - \frac{K_s}{J_R} \theta_R + \frac{1}{J_R} \Gamma_{el}, \quad (24)$$

$$s\Gamma_{Le} = 0. \quad (25)$$

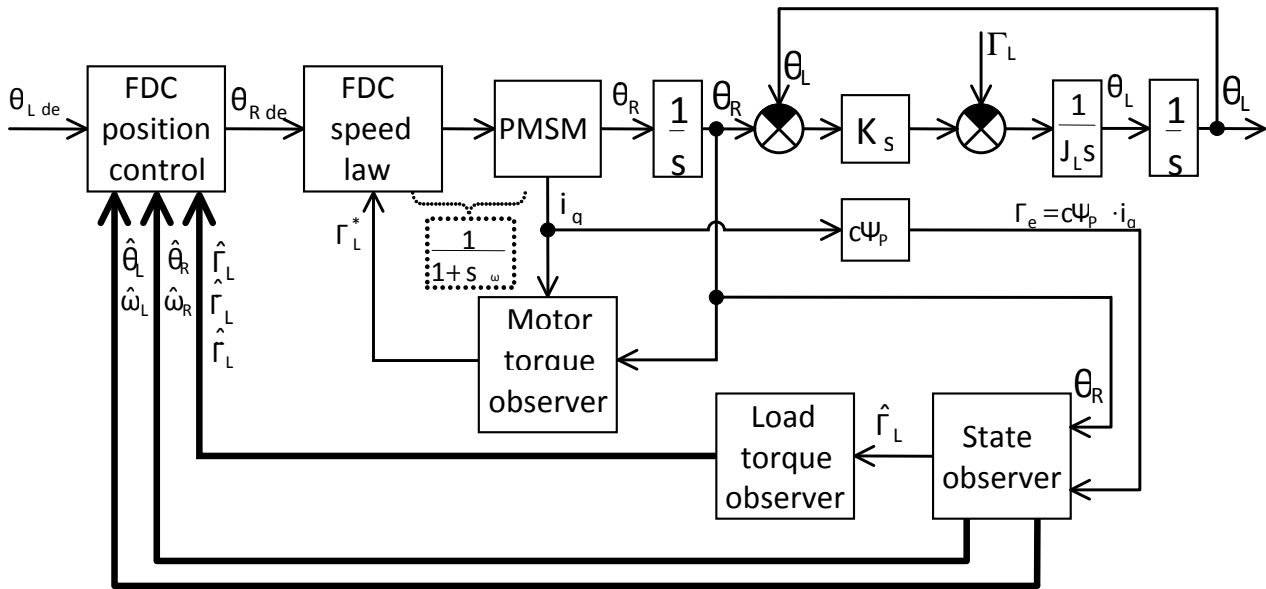


Fig. 4. Overall position control system block diagram

Rewritten in matrix form:

$$\begin{bmatrix} \dot{\theta}_L \\ \dot{\theta}_R \\ \dot{\omega}_L \\ \dot{\omega}_R \\ \dot{\Gamma}_{Le} \end{bmatrix} = \begin{bmatrix} 0 & 0 & 1 & 0 & 0 \\ 0 & 0 & 0 & 1 & 0 \\ -a_1 & a_1 & 0 & 0 & -a_2 \\ a_3 & -a_3 & 0 & 0 & 0 \\ 0 & 0 & 0 & 0 & 0 \end{bmatrix} \begin{bmatrix} \theta_L \\ \theta_R \\ \omega_L \\ \omega_R \\ \Gamma_{Le} \end{bmatrix} + [0 \ 0 \ 0 \ a_4 \ 0]^T \Gamma_{el}, \tag{26}$$

where constants are defined, $a_1 = K_s/J_L$, $a_2 = 1/J_L$, $a_3 = K_s/J_R$ and $a_4 = 1/J_R$.

Observer's equation in matrix form is:

$$\begin{bmatrix} \dot{\hat{\theta}}_L \\ \dot{\hat{\theta}}_R \\ \dot{\hat{\omega}}_L \\ \dot{\hat{\omega}}_R \\ \dot{\hat{\Gamma}}_{Le} \end{bmatrix} = \begin{bmatrix} 0 & 0 & 1 & 0 & 0 \\ 0 & 0 & 0 & 1 & 0 \\ -a_1 & a_1 & 0 & 0 & -a_2 \\ a_3 & -a_3 & 0 & 0 & 0 \\ 0 & 0 & 0 & 0 & 0 \end{bmatrix} \begin{bmatrix} \hat{\theta}_L \\ \hat{\theta}_R \\ \hat{\omega}_L \\ \hat{\omega}_R \\ \hat{\Gamma}_{Le} \end{bmatrix} + \begin{bmatrix} 0 \\ 0 \\ 0 \\ a_4 \\ 0 \end{bmatrix} \Gamma_{el} + \begin{bmatrix} k_{\theta 1} \\ k_{\theta 2} \\ k_{\omega 1} \\ k_{\omega 2} \\ k_{\Gamma 1} \end{bmatrix} (\theta_R - \hat{\theta}_R). \tag{27}$$

Equation of the 'dynamical error system' is obtained by subtracting observer equations (27) from its real time

model (26):

$$\begin{bmatrix} \dot{\varepsilon}_{\theta L} \\ \dot{\varepsilon}_{\theta R} \\ \dot{\varepsilon}_{\omega L} \\ \dot{\varepsilon}_{\omega R} \\ \dot{\varepsilon}_{\Gamma_{Le}} \end{bmatrix} = \begin{bmatrix} 0 & -k_{\theta 1} & 1 & 0 & 0 \\ 0 & -k_{\theta 2} & 0 & 1 & 0 \\ -a_1 & a_1 - k_{\omega 1} & 0 & 0 & -a_2 \\ a_3 & -a_3 - k_{\omega 2} & 0 & 0 & 0 \\ 0 & k_{\Gamma 1} & 0 & 0 & 0 \end{bmatrix} \begin{bmatrix} \varepsilon_{\theta L} \\ \varepsilon_{\theta R} \\ \varepsilon_{\omega L} \\ \varepsilon_{\omega R} \\ \varepsilon_{\Gamma_{Le}} \end{bmatrix} \tag{28}$$

To ensure convergence of the state estimates toward the real states the gains of observer, $k_{\theta 1}$, $k_{\theta 2}$, $k_{\omega 1}$, $k_{\omega 2}$ and $k_{\Gamma 1}$ must be chosen in such a way that dynamical error system satisfies condition for $t \rightarrow \infty \varepsilon_i(t) \rightarrow 0$. Such convergence is guaranteed if the eigenvalues of the system matrix have negative real parts.

$$\det \begin{bmatrix} \lambda & k_{\theta 1} & -1 & 0 & 0 \\ 0 & \lambda + k_{\theta 2} & 0 & -1 & 0 \\ a_1 & k_{\omega 1} - a_1 & \lambda & 0 & a_2 \\ -a_3 & k_{\omega 2} + a_3 & 0 & \lambda & 0 \\ 0 & -k_{\Gamma 1} & 0 & 0 & \lambda \end{bmatrix} = \lambda^5 + \lambda^4 k_{\theta 2} + \lambda^3 (a_3 + k_{\omega 2}) + \lambda^2 a_3 k_{\theta 1} + \lambda (a_1 k_{\omega 2} + a_3 k_{\omega 1}) + a_2 a_3 k_{\Gamma 1}. \tag{29}$$

Under assumption of collocations of all five error system eigenvalues at $\lambda = -\omega_0$ (the observers settling time can be determined by formula, (13), which for $n = 5$ results in $T_{sO} = 9/\omega_0$), the desired characteristic equation has form:

$$(s + \omega_0)^5 = s^5 + 5\omega_0 s^4 + 10\omega_0^2 s^3 + 10\omega_0^3 s^2 + 5\omega_0^4 s + \omega_0^5. \tag{30}$$

Comparing the coefficients of the same degree in (29)

and (30) yields the required values of observer gains:

$$\begin{aligned}
 k_{\Gamma 1} &= \omega_0^5 / a_2 a_3 k_{\theta 2} = 5\omega_0 k_{\omega 2} = 10\omega_0^2 - a_1 - a_3 k_{\theta 1} \\
 &= (10\omega_0^3 - a_1 k_{\theta 2}) / a_1 k_{\omega 1} = (5\omega_0^4 - a_1 k_{\omega 2}) / a_3.
 \end{aligned}
 \tag{31}$$

Although the load torque is assumed constant in the formulation of the observer real time model, its estimate Γ_{Le} , will follow a time varying load torque and will do so more faithfully as ω_0 is enlarged with respect of the computational step. Block diagram of load torque observer 1 is shown in Figure 5.

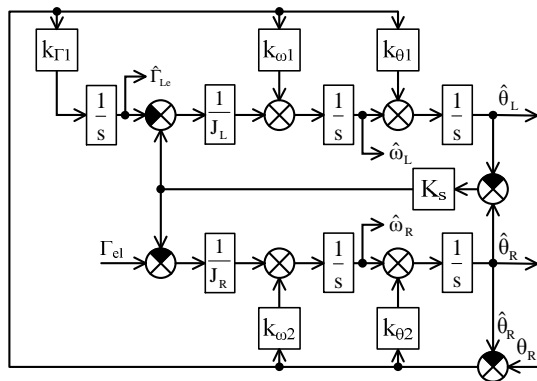


Fig. 5. Block diagram of state variables observer

Correct function of observer was verified for estimation of uncontrolled flexible coupling state variables when constant torque, $\Gamma_{el} = 2 \text{ Nm}$ was applied at $t = 0.1 \text{ s}$ which was followed by equivalent load torque $\Gamma_{Le} = 2 \text{ Nm}$ at $t = 0.5 \text{ s}$. Settling time of the observer was chosen as $T_{sO} = 50 \text{ ms}$. Simulation results are shown in Figure 6.

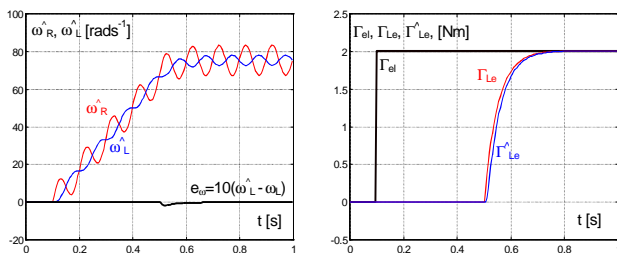


Fig. 6. Simulation results of state variables observer

3.2 Load Torque Derivatives Observer

To produce the first and second derivative of load torque required by the derived control law (19), a similar observer to the previous one was designed. In this case the second derivative of external torque load is treated as if it is constant provided that its change over a period equal to the

observer correction loop settling time T_{so} , is negligible. System state equations in matrix form are as follows:

$$\begin{bmatrix} s\Gamma_{Le} \\ s\dot{\Gamma}_{Le} \\ s\ddot{\Gamma}_{Le} \end{bmatrix} = \begin{bmatrix} 0 & 1 & 0 \\ 0 & 0 & 1 \\ 0 & 0 & 0 \end{bmatrix} \begin{bmatrix} \Gamma_{Le} \\ \dot{\Gamma}_{Le} \\ \ddot{\Gamma}_{Le} \end{bmatrix}. \tag{32}$$

If the error between load torque as the output of state variables observer and load torque estimated in the derivatives observer defined as $e = \Gamma_{Le} - \hat{\Gamma}_{Le}$ is added with proper gain into every observer correction loop, then the torque derivatives observer equations are as follows:

$$\begin{bmatrix} s\hat{\Gamma}_{Le} \\ s\dot{\hat{\Gamma}}_{Le} \\ s\ddot{\hat{\Gamma}}_{Le} \end{bmatrix} = \begin{bmatrix} 0 & 1 & 0 \\ 0 & 0 & 1 \\ 0 & 0 & 0 \end{bmatrix} \begin{bmatrix} \hat{\Gamma}_{Le} \\ \dot{\hat{\Gamma}}_{Le} \\ \ddot{\hat{\Gamma}}_{Le} \end{bmatrix} + \begin{bmatrix} k_1 \\ k_2 \\ k_3 \end{bmatrix} (\Gamma_{Le} - \hat{\Gamma}_{Le}). \tag{33}$$

Subtraction of (33) from (32) gives dynamical error system, which has the form

$$\begin{bmatrix} \dot{\epsilon}_1 \\ \dot{\epsilon}_2 \\ \dot{\epsilon}_3 \end{bmatrix} = \begin{bmatrix} -k_1 & 1 & 0 \\ -k_2 & 0 & 1 \\ -k_3 & 0 & 0 \end{bmatrix} \begin{bmatrix} \epsilon_1 \\ \epsilon_2 \\ \epsilon_3 \end{bmatrix}. \tag{34}$$

Convergence of dynamical error system for $t \rightarrow \infty$ $\epsilon_i(t) \rightarrow 0$ is guaranteed for the eigenvalues of the system matrix with negative real parts. Under assumption of all three eigenvalues collocations at $\lambda = -\omega_0$ (using (13) for $n = 3$ results in observer's settling time $T_{so} = 6/\omega_0$). Comparing the desired third order characteristic equation with equation of system matrix eigenvalues results in the following gains of observer correction loops:

$$s^3 + 3\omega_0 s^2 + 3\omega_0^2 s + \omega_0^3 = \lambda^3 + \lambda^2 k_1 + \lambda k_2 + k_3, \tag{35}$$

$$k_3 = \omega_0^3, k_2 = 3\omega_0^2, k_1 = 3\omega_0. \tag{36}$$

Load torque observer block diagram of is shown in Fig. 7.

Figure 8 illustrates correct function of the observer when the numerically computed first and second derivatives of exponential load torque are compared with the derivatives gained from the load torque observer.

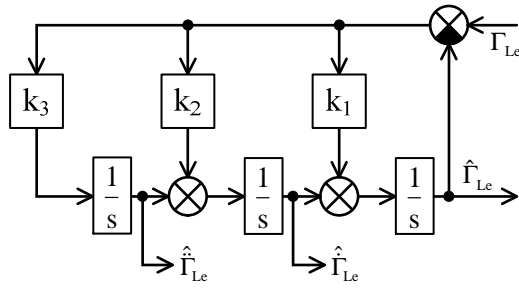


Fig. 7. Load torque observer

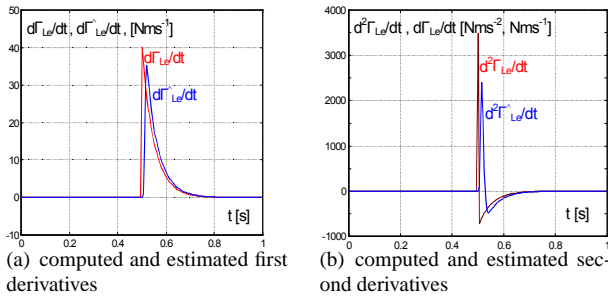


Fig. 8. Computed and estimated the first and second derivative

3.3 Motor Load Torque Observer

Load torque on the motor shaft needed for FDC speed control is estimated in ‘motor load observer’. Due to the fact that the form of $\Gamma_{Ls}(t)$ is unknown, its differential equations cannot be formed. Motor load torque Γ_{Ls} is therefore treated as state variable, which is constant provided that its change over a period equal to the observer correction loop settling time T_{su} is negligible. Thus, the observer real time model is based on (1) and (2) augmented by a new state equation, $-d\Gamma_{Ls}/dt = 0$.

$$\frac{d\theta_R^*}{dt} = \omega_R^* + k_\theta e_\theta^*, \quad (37)$$

$$\frac{d\omega_R^*}{dt} = \frac{1}{J_R} [c \Psi_{PM} i_q - \Gamma_{Ls}^*] + k_\omega e_\omega^*, \quad (38)$$

$$\frac{-d\Gamma_{Ls}^*}{dt} = 0 + k_\Gamma e_\Gamma^*. \quad (39)$$

Mathematical description of the observer is available in [13] therefore to save some space only the final comparison of characteristic polynomial of the observer’s transfer function with desired characteristic equation is given:

$$s^3 + k_\theta s^2 + k_\omega s + \frac{k_\Gamma}{J_R} = s^3 + s^2 \frac{18}{T_{su}} + s \frac{108}{T_{su}^2} + \frac{216}{T_{su}^3}. \quad (40)$$

Observer’s gains k_θ , k_ω and k_Γ for a specified correction loop settling time, T_{so} are as follows:

$$k_\theta = 3\omega_0, k_\omega = 3\omega_0^2, k_\Gamma = J_R\omega_0^3. \quad (41)$$

So with sufficiently small settling time of observer T_{su} , the observer, which is shown in Figure 9, produces a net load torque estimate, $\Gamma_{LR}^*(t)$ able to track real load torque, $\Gamma_{Ls}(t)$ with very small and defined dynamic lag.

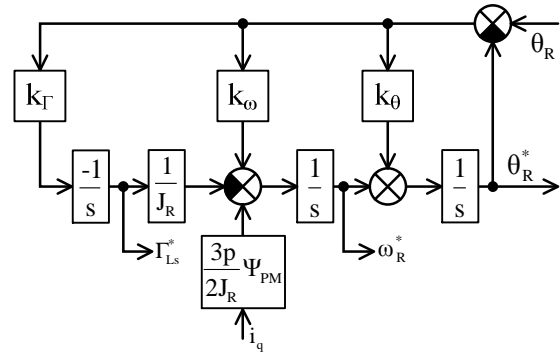


Fig. 9. Block diagram of motor load torque observer

Correct function of the motor load torque observer illustrates Figure 10. Subplot a) shows the real and estimated rotor speed including the difference between them magnified 5x. Applied and estimated load torque on the shaft of the motor is shown in subplot b) including the error between them. In spite of dynamic lag of the estimated variable, which can be seen in this subplot, the observer produces a correct estimate of load torque on the shaft of the motor demanded by FDC of rotor speed.

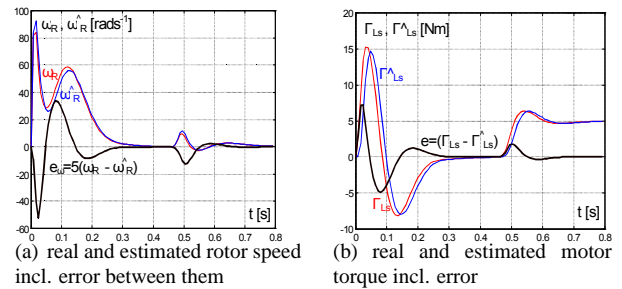


Fig. 10. Real and estimated rotor speed and load torque

4 OVERALL CONTROL SYSTEM VERIFICATION

Simulations of the proposed FDC system followed by verification of the designed observers via experimental data collected for control of flexible coupling with two position sensors described in [12] were carried out to verify overall performances of the proposed control of flexible coupling with single position sensor on motor side.

Simulation results of FDC of the load position are presented in Figure 11 and Figure 12. Verification of the observers' operation from measured data is shown in Figure 13.

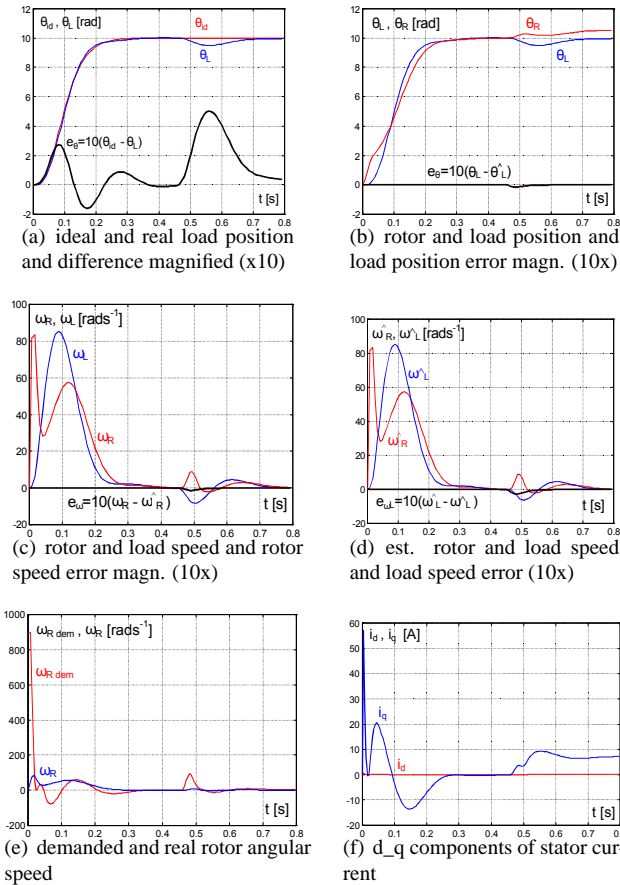


Fig. 11. Simulation results for position control of the drive with flexible coupling

The computational step of simulations is $h = 1 \cdot 10^{-4} s$, which corresponds to the sampling frequency achieved during a previous implementation of the algorithm for FDC of load position. All the simulations presented are carried out with zero initial state variables. A step load angle demand $\theta_{L\ dem} = 10$ rad with settling time $T_{s\theta} = 0.2$ s was applied to investigate response of the FDC based control system. An external load torque with exponential increase given as $\Gamma_{Le} = 5(1 - e^{-t/0.05})$ is applied at $t = 0.5$ s, being zero for the time interval $t < 0.5$ s. The settling time of the state and load torque observer were chosen as $T_{sO} = T_{so} = 12.5$ ms, while settling time of motor torque observer is set as $T_{su} = 1.5$ ms respectively.

Subplot (a) of Fig. 11 shows the ideal response and response of the control system to the step load position demand, $\theta_{L\ dem} = 10$ rad. including magnified difference

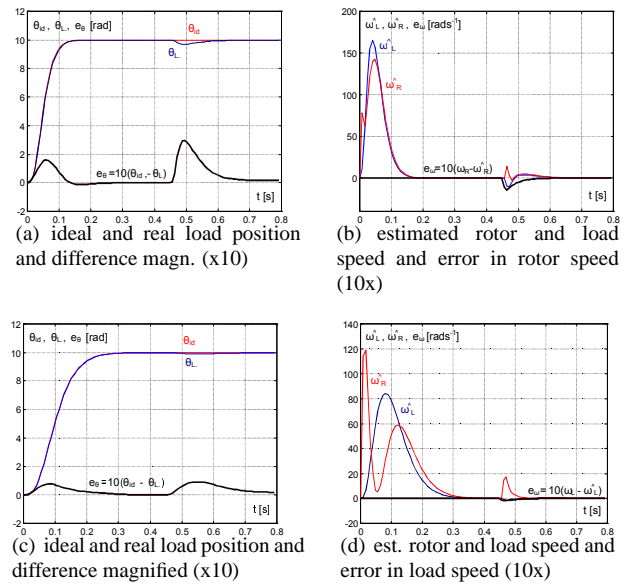


Fig. 12. Simulation results for position control of the drive with various moment of inertia

between them (10x). The realisation of the prescribed position dynamics is very accurate, which is clear from the magnified difference. Also the prescribed settling time is precisely kept because the load position, $\theta_L(t)$ passes through 9.5 radian at a time very close to 0.2s. Subplot (b) shows load position and rotor position together with the error between real and estimated load position (*magnified 10x*). From this subplot can be seen also that in the steady state, the motor electrical torque is transmitted via the torsion spring to counteract the external load torque applied to the load mass. This entails a constant torsional deflection of the spring, which is evident from the constant difference between θ_R and θ_L occurring just after the load torque achieves its steady state.

Subplot (c) shows the angular velocities of the rotor and load as functions of time together with the difference between real and estimated rotor speed (*magnified 10x*). This subplot illustrate that the acceleration period is followed by the deceleration one, as expected. Correct function of 'states observer' is shown in subplot (d) where the estimated rotor and load speeds are shown including the difference between real and estimated load speed (*magnified 10x*). It can be seen that the errors in estimates occur during transients only.

Demanded rotor speed as an input to FDC speed algorithm together with real response of the motor speed is shown in subplot (e). The PMSM i_q -current torque component is shown in subplot (f) while the i_d -current component is kept at zero value up to the nominal motor speed satisfying condition for vector control of PMSM.

Figure 12 shows simulation results of robustness investigation when two different moments of load inertia were applied ($J_{L1} = 0.75 \cdot 10^{-3} \text{ kgm}^2$ and $J_{L2} = 12 \cdot 10^{-3} \text{ kgm}^2$) while the moment of motor inertia ($J_R = 3 \cdot 10^{-3} \text{ kgm}^2$) was constant. The corresponding encastre natural frequency ($v_1 = 109.5 \text{ rads}^{-1}$ and $v_2 = 27.4 \text{ rads}^{-1}$) and free natural frequency ($w_1 = 122.5 \text{ rads}^{-1}$ and $w_2 = 61.2 \text{ rads}^{-1}$) were determined using (10) for spring constant $K_s = 9 \text{ Nmrad}^{-1}$. To achieve satisfactory results the prescribed settling time for the drive with higher free natural frequency was set to $T_{s\theta} = 0.1 \text{ s}$ and for lower free natural frequency was set to $T_{s\theta} = 0.2 \text{ s}$.

Simulation results for both chosen moments of inertia are compressed into two subplots. Subplots (a) and (b) show the ideal response and response of the control system to the step load position demand, $\theta_{L \text{ dem}} = 10 \text{ rad}$ with prescribed settling time of $T_{s\theta 1} = 0.1 \text{ s}$ and $T_{s\theta 2} = 0.2 \text{ s}$ including difference between them (*magnified 10x*). Position response of the drive including prescribed settling time is accurate, which is clear from the magnified difference between ideal and real position response. Subplots (c) and (d) show the estimated velocities of the rotor and load as functions of time together with the difference between real and estimated rotor speed (*magnified 10x*). These results also confirm correct function of the state observer under various load conditions.

Correct operation of the designed observers was investigated using data collected during control of flexible coupling with two position sensors. Results are shown in Figure 13. Experiments were carried out for load angle demand $\theta_{L \text{ dem}} = 2\pi \text{ rad}$ with settling time $T_{s\theta} = 0.2 \text{ s}$ and with exponential increase of external load torque and spring constant $K_s = 24 \text{ Nmrad}^{-1}$.

Subplot (a) of Figure 13 shows measured rotor position for whole data collecting interval. Measured components of stator current are shown in subplot (b). Proper function of state observer, which exploits both measured data as the inputs, shows subplot (c) where measured and observed load position are shown including error between them (*magnified 10x*). Subplot (d) shows estimated rotor and load angular speed. Estimated load position together with both estimated speeds serve as the inputs of FDC algorithm to control load position.

One of the output of state variables observer is estimated load torque, which is utilized in FDC of load position, as well as creates input for load torque derivatives observer. Estimation of the first and second derivative of load torque shows subplot (e). This way proper function of load torque derivatives observer was confirmed.

Presented simulation results and preliminary investigations of correct observers operation confirmed possibility to control load angle with single position sensor on the

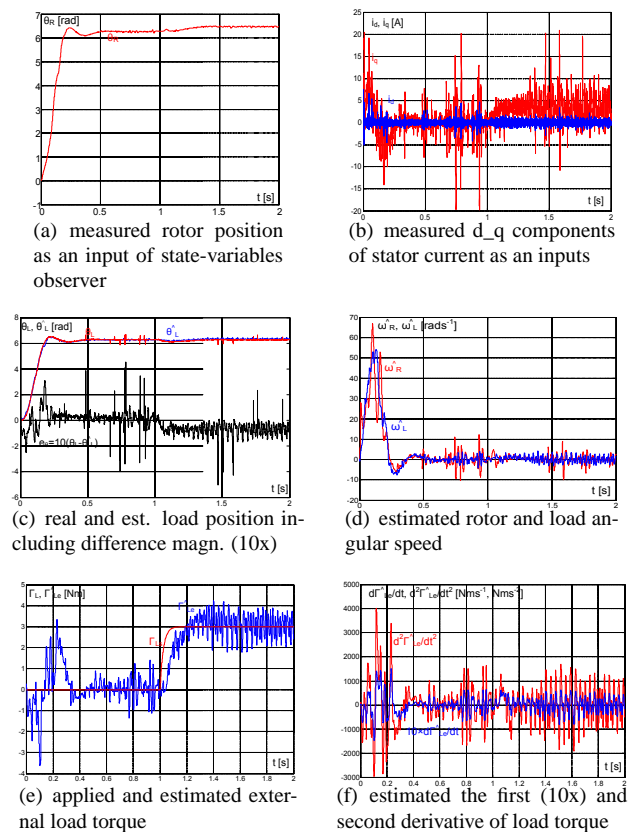


Fig. 13. Comparison of measured and estimated control variables by the designed observers

motor side using FDC. An important observation based on simulation results is that the mechanical oscillations are completely damped and the peak of transient error if compared with ideal transfer function doesn't exceed 0.5 rad allowing position control of the load with moderate accuracy.

5 CONCLUSION

A position control system based on the principles of 'Forced Dynamics Control' for electric drives with flexible couplings has been presented and verified by simulations. Simulation results confirmed that the proposed position control system can be made to follow the prescribed ideal closed-loop dynamics with moderate precision in spite of the presence of flexible modes and external torque. Simulation results also confirm accomplishment of the vector control conditions by keeping direct axis current to small proportion.

Implementation of three observers enables control of load position with fair precision and to eliminate the load position sensor. Preliminary tests of observers based on previously measured data has shown their capability to

provide estimates of all state variables for control algorithm including rotor torsion torque, Γ_{Ls} , and external load torque, Γ_{Le} respectively. The same is valid about estimation of load torque the first and second derivatives required by the position control algorithm.

Simulation results indicate that the designed position control system exhibits the desired robustness and therefore warrants further development and experimental investigation.

ACKNOWLEDGMENT

The authors wish to thank for support to Slovak Grant Agency VEGA and R&D operational program Centre of excellence of power electronics systems and materials for their components II. No. OPVaV-2009/2.1/02-SORO, ITMS 26220120046 funded by European regional development fund (ERDF).

REFERENCES

- [1] A. Isidori, *Nonlinear Control Systems*, London, Springer-Verlag, UK, 1995.
- [2] I. Boldea, S. A. Nasar, *Vector Control of AC Drives*. 2nd ed., Boca Raton, FL., CRC Press, 1992.
- [3] D. W. Novotny, T. A. Lipo, *Vector Control and Dynamics of AC drives*, New York, Oxford University Press, 1996.
- [4] J. Vittek, S. J. Dodds, R. Perryman, M. Rapšák, "Forced Dynamics Control of Electric Drives employing PMSM with Flexible Coupling" Australasian Universities Power Engineering Conference AUPEC 2007, Perth, Australia, dec. 2007, CD-Rom.
- [5] J. Vittek, P. Briš, P. Makyš, M. Štulrajter, "Control of Flexible Drive with Permanent Magnet Synchronous Motor employing Forced Dynamics", Proceedings of EPE-PEMC 2008 conf., Sept. 2008, Poznan, Poland, CD-Rom, pp. 2242-2249.
- [6] G. Zhang, J. Furusho, "Speed control of two-inertia system by PI/PID control", *IEEE Trans. on Industrial Electronics*, vol. 47, no. 3, 2000, pp. 603-609.
- [7] S. Thomsen, N. Hoffmann, F. W. Fuchs, "PI control, PI-based state space control, and model-based predictive control for drive systems with elastically coupled loads-A comparative study", *IEEE Transactions on Industrial Electronics* Vol. 58 (8), 2011, pp. 3647-3657.
- [8] B. U. Nam, H. S. Kim., H. J. Lee, , D. H. Kim, "Optimal Speed Controller Design of the Two-Inertia Stabilization System", *International Journal of Computer and Information Engineering* 2009, pp. 41-46.
- [9] D. J. Shin, U. J. Hah, J. H. Lee, "An Observer Design for 2 Inertia Servo Control System", Proceedings of the IEEE International Symposium on Industrial Electronics ISIE '99, CD-Rom.
- [10] S. J. Dodds, K. Szabat, "Forced Dynamic Control of Electric Drives with Vibration Modes in the Mechanical Load", in Proceedings of the International conf. EPE-PEMC'06, Portorož, Slovenia, 2006, CD-Rom.
- [11] K. Szabat, T. Orłowska-Kowalska, "Damping of the Torsional Vibration in Two-Mass Drive System Using Forced Dynamic Control", . The International Conference on Computer as a Tool, EUROCON 2007, pp. 1712 – 1717.
- [12] J. Vittek, P. Bris, P. Makys, M. Stulrajter, "Forced Dynamics Control of PMSM Drives with Torsion Oscillations", *COMPEL - The International Journal for Computation and Mathematics in Electrical and Electronic Engineering* Vol. 29, No. 1, 2010, pp.187-204.
- [13] J. Vittek, S. J. Dodds, *Forced Dynamics Control of Electric Drives*, Zilina, SK, EDIS, <http://www.kves.uniza.sk>, (*E-learning*), 2003.
- [14] S. J. Dodds, "Settling Time Formulae for the Design of Control Systems with Linear Closed Loop Dynamics", International conf. AC&T'07 - Advances in Computing and Technology, University of East London, UK, 2007.
- [15] W. Leonhard, "*Control of Electrical Drives*", 2nd ed., Springer, Berlin 2001.
- [16] K. Bose, "*Power Electronics and Variable Frequency Drives – Technology and Applications*", Institute of Electrical and Electronics Engineers, New York 1997.
- [17] K. Ohnishi, M. Morisawa, "Motion control taking environmental information into account", in Proceedings of the EPE PEMC'02 International conf., Cavtat, Croatia, 2002, CD-Rom.
- [18] O. Aguilar, A. G. Loukianov, J. M. Canedo, "Observer-based Sliding Mode Control of Synchronous Motor:", in Proceedings of the intern. IFAC'02 congress on Automatic Control, Guadalajara, Mexico, CD-Rom, 2002.
- [19] S. Brock, J. Deskur, K. Zawirski, "Robust Speed and Position Control of PMSM using Modified Sliding Mode Method", in Proceedings of the International conf. EPE-PEMC 2000, Kosice, Slovakia, vol. 6, pp. 6-29–6-34.

- [20] V. Comnat., M. Cernat., F. Moldoveanu, R. Ungar, "Variable Structure Control of Surface Permanent Magnet Synchronous Machine", International conf. PCIM 1999 Nurnberg, Germany, pp. 351-356, CD-Rom.
- [21] D. Perdukova, P. Fedor, J. Timko, "Modern Methods of Complex Drives Control", Acta Technica ČSAV, vol. 49, Prague, Czech Republic, pp. 31-45, 2004.
- [22] S. Ryvkin, D. Izosimov, E. Palomar-Lever, "Digital Sliding Mode Based References Limitation Law for Sensorless Control of an Electromechanical Systems", *Journal of Physics* 2005, IOP Publ. Ltd, series 23, pp. 192-201.
- [23] M. Yang, H. Hu, H., D. G. Xu, "Cause and suppression of mechanical resonance in PMSM servo system", *Dianji yu Kongzhi Xuebao/Electric Machines & Control*, Vol. 16, (1), 2012, pp. 79-84.
- [24] T. Pajchrowski, "Robust control of PMSM system using the structure of MFC", *COMPEL - The International Journal for Computation and Mathematics in Electrical and Electronic Engineering*, Vol. 30, (3), 2011, pp. 979-995.



Ján Vittek received his Ph.D. degree from the Technical University of Transport Zilina in 1979. After two years service in CZ Railroads he joined Faculty of Electrical Engineering of the University of Transport and Communications in Zilina. In 1997 he became a professor for 'Electric Traction and Electric Drives'. He is responsible for the development of Electric Drives division in the department of Power Electrical Systems. During period 1998-2008 he was several times appointed to the position of Visiting Professor of the School

of Computing and Technology, University of East London, UK as the reflection of long-term research co-operation. His research interests are control of electric drives, electronic energy conversion, electric traction (including locomotive drives and traction power supply) and applied robust control.



Vladimír Vavruš received the MSc. degree in Electrical and Electronic Engineering from University of Zilina in 2005 and thereafter he began PhD study at the same place. He received his PhD degree in 2009 and he is currently working as a researcher at the Faculty of Electrical Engineering, Zilina University. His research interests cover control of electric drives with special interest in strategies for control of linear motors. He cooperates on the development of electronic hardware for different industrial applications using digital signal processors and power PC as well.



Peter Briš received the MSc. degree in Electrical and Electronic Engineering from University of Zilina in 2007 and thereafter he began PhD study at the same place. He received his PhD degree in 2011 and he is currently working as a researcher at Railway Repairs and Machineries, Vrútky. His research interests cover control of electric drives with special interest in energy saving control algorithms and robust control methods for drives with flexible coupling.



Lukáš Gorel received his master degree in power electrical engineering from faculty of electrical engineering, University of Zilina in 2011. Currently he is continuing his study as a doctoral student in the field of 'electric drives' at the same faculty. His research interests are control of electric drives, position sensors sensitivity and control of electric drives with flexible coupling.

AUTHORS' ADDRESSES

Ján Vittek, Prof.

Vladimír Vavruš, Ph.D.

Peter Briš, Ph.D.

Lukáš Gorel, M.Sc.

Department of Power Electrical Systems,

Faculty of Electrical Engineering,

University of Zilina,

Univezitna 1, Velky diel, 010 26 Zilina, Slovak

Republic

e-mail: jan.vittek@fel.uniza.sk

vladimir.vavrus@kves.uniza.sk

peter.bris@gmail.com

lukas.gorel@kves.uniza.sk

Received: 2012-01-09

Accepted: 2012-11-21